IX CONGRESSO BRASILEIRO DE
ENGENHARIA E CIÊNCIAS TÉRMICAS

9th BRAZILIAN CONGRESS OF THERMAL
ENGINEERING AND SCIENCES

Paper CIT02-0800

A Three-Dimensional Isoparametric Finite-Element Discretization Scheme to Treat the Interfacial Thermal Resistance in Composite Materials

C. F. Matt
Laboratório de Transmissão e Tecnologia do Calor - LTTC/DEM/EE/COPPE/UFRJ, Universidade Federal do Rio de Janeiro, Caixa Postal 68503, CEP: 21945-970, Rio de Janeiro, RJ, Brasil
cftmatt@lttc.coppe.ufrj.br

M. E. Cruz
Laboratório de Transmissão e Tecnologia do Calor - LTTC/DEM/EE/COPPE/UFRJ, Universidade Federal do Rio de Janeiro, Caixa Postal 68503, CEP: 21945-970, Rio de Janeiro, RJ, Brasil
manuel@serv.com.ufrj.br

Abstract. *Composites are among the most important and frequently used materials. The determination of macroscopic thermal properties of composites is of great engineering interest. It is frequent in the literature to calculate the effective conductivity of composites assuming that the individual constituents have a perfect thermal contact. In reality, that is not the case, and one has to account for the interfacial thermal resistance which is almost inevitably present between the constituents. In this paper, we develop a new three-dimensional isoparametric finite-element discretization scheme to treat the interfacial thermal resistance in composite materials. We demonstrate the validity and flexibility of our scheme by effecting truly three-dimensional sample calculations of the effective conductivity of an ordered-array composite, for which analytical results are known. The scheme presented here has the distinct advantage of being applicable to complex and realistic microstructures.*

Keywords: *Heat conduction, composite materials, finite elements, interfacial thermal resistance.*

1. Introduction

Composite materials are relatively easy to fabricate, and are versatile with respect to mechanical and thermal properties. As a consequence, they are among the most important and frequently used materials. The detailed study of the local transport of heat in composite materials is an essentially impossible task, due to their complex microstructures. Engineering analyses thus aim to determine the global, effective thermal conductivity of composites in terms of their microstructures and relevant physical parameters.

Frequently, due to mathematical simplifications, the effective conductivity of composites is calculated assuming that the individual constituents have a perfect thermal contact. In reality, perfect contact is not afforded by standard manufacturing processes, and one has to account for the interfacial thermal resistance which is almost always present between the constituents. In this paper, we develop a new three-dimensional isoparametric finite-element discretization scheme to treat the interfacial thermal resistance in composite materials. The general scheme presented here has the advantage of being applicable to complex and realistic microstructures.

The paper is organized as follows. In section 2, we briefly review the pertinent literature. In section 3, we describe the multiscale heat conduction problem in a composite material with interfacial thermal resistance between the constituents, and write the appropriate continuous cell problem which has to be solved, to be able to calculate the effective conductivity. In section 4, we present in detail our new three-dimensional isoparametric finite-element discretization scheme to deal with the surface integral term which arises due to the interfacial thermal resistance. In section 5, we demonstrate the validity and flexibility of our scheme by presenting the results for a case study: we effect truly three-dimensional sample calculations of the effective conductivity of an ordered-array composite, for which analytical results are known. Finally, we wrap up the paper with conclusions and comments on future work.

2. Brief Literature Review

Comprehensive reviews of analytical and experimental techniques for the study of heat conduction in composite materials are presented by Mirmira (1999), Mirmira and Fletcher (1999), and Furmañski (1997). In general, analytical (e.g., Hasselman and Johnson, 1987; Perrins et al., 1979) and phenomenological (e.g., Every et al., 1992; Benveniste, 1987) treatments of heat conduction in composites are restricted to simple microstructures and dilute concentrations, or to the validity of self-consistent assumptions. Computational approaches, reviewed by Cruz (2001), are better suited to treat more complex geometries and phenomena relative to analytical studies. Different numerical schemes have been employed to investigate heat conduction in composite materials: finite elements (Matt and Cruz, 2001; Rolfes and Hammerschmidt, 1995; Cruz and Patera, 1995), finite differences (James and Keen, 1985) and boundary elements (Ingber et al., 1994). An alternative to exact analytical treatments is statistical bound methods, reviewed by Torquato (1991). The objective of these methods is to determine upper and lower bounds for the effective property of interest, based on a description of the composite microstructure via correlation functions. In all these studies, the effective thermal conductivity is determined in terms of the microstructure and individual physical properties of the constituents.

Because most fabrication processes of composite materials do not ensure a perfect thermal contact between the constituent phases, the effective thermal conductivity also depends on the interfacial thermal resistance, or contact resistance, between the continuous (matrix) and the dispersed phases. This interfacial resistance is due to poor chemical and/or mechanical adherence, caused by different thermal expansion coefficients of the phases, and the presence of roughness, waving and impurities at the interface (Cheng and Torquato, 1997; Lipton and Vernescu, 1996; Fletcher, 1988). Physically, the contact resistance tends to thermally insulate the dispersed phase, and may dramatically reduce the conduction capacity of the composite material. Despite the significant influence of the contact resistance on the effective conductivity of the composite, the authors are unaware of any three-dimensional numerical study which attempts to account for this effect.

The interface between the phases of a composite is usually modeled as a surface of zero thickness, and the contact resistance is defined as the ratio of the temperature jump to the heat flux at the interface. The evaluation of the contact resistance between surfaces of various geometries, finish, materials and modes of deformation of their asperities and substrates is the subject of a large number of investigations (Fletcher, 1988). Previous analytical (Cheng and Torquato, 1997; Lipton and Vernescu, 1996; Auriault and Ene, 1994; Hasselman and Johnson, 1987), phenomenological (Every et al., 1992; Benveniste, 1987), and computational (Rocha and Cruz, 2001) studies of heat conduction in composite materials, however, regard the interfacial resistance as an independent (prescribed) uniform parameter; here, though not a necessary assumption, we adopt this same approach. Specifically, we extend in two important directions the finite-element computational procedure recently developed by Rocha and Cruz (2001), to treat conduction in unidirectional composites with contact resistance: first, we add one more dimension, and second, we employ isoparametric quadratic discretization. While the implementation of this new procedure is significantly more complicated, it can be applied to realistic three-dimensional geometries of composite materials.

3. The Continuous Cell Problem

The problem considered here is heat conduction in a multiscale periodic composite, Ω, composed of a dispersed phase of geometric domain Ω_d and thermal conductivity k_d, and a continuous phase of geometric domain Ω_c and thermal conductivity k_c. There is a uniform interfacial thermal resistance r, or interfacial thermal conductance $h \equiv 1/r$, between the phases. The conductivity ratio α is defined as $\alpha \equiv k_d/k_c$, $k_d, k_c > 0$. It is assumed that the constituent phases are solid, homogeneous and isotropic. An external temperature gradient of magnitude $\Delta T/L$ is imposed over the *macroscale* L of Ω. The smallest length scale of Ω is the characteristic size d of the dispersed phase, called the *microscale*. The *mesoscale* λ ($d < \lambda \ll L$) is the characteristic length of the periodic cell, Ω_{pc}, of volume λ^3; we denote by $\Omega_{pc,c}$ and $\Omega_{pc,d}$ the subdomains of Ω_{pc} occupied by the continuous and dispersed phases, respectively. The parameter $\epsilon \equiv \lambda/L$ is the ratio of two natural length scales of the problem, and is assumed to be much less than unity. The concentration c, or dispersed-phase volume fraction, is defined as the ratio of the volume of $\Omega_{pc,d}$ and the volume of Ω_{pc}.

The continuous formulation of the heat conduction cell problem in Ω_{pc} is obtained from the original multiscale problem in Ω by applying the method of homogenization (Auriault and Ene, 1994; Furmański, 1997; Auriault, 1991; Bensoussan et al., 1978). Rocha and Cruz (2001) have derived in detail the general nondimensional variational formulation of the cell problem for finite values of the Biot number, $\mathrm{Bi} \equiv h\lambda/k_c = O(\epsilon^0)$. For our purposes in this paper, it suffices to assume that the composite is isotropic. Defining χ as the periodic cell temperature field, using λ and ΔT as the characteristic length and temperature scales, respectively, and adopting the summation convention over repeated indices, the weak form of the cell problem for an isotropic composite is given by

$$\int_{\Omega_{pc,c}} \frac{\partial \chi^c}{\partial y_j}\frac{\partial v^c}{\partial y_j} d\mathbf{y} + \int_{\Omega_{pc,d}} \alpha \frac{\partial \chi^d}{\partial y_j}\frac{\partial v^d}{\partial y_j} d\mathbf{y} + \int_{\Gamma} \mathrm{Bi}[v]_\Gamma [\chi]_\Gamma d\mathbf{s} = \int_{\Omega_{pc,c}} \frac{\partial v^c}{\partial y_1} d\mathbf{y} + \int_{\Omega_{pc,d}} \alpha \frac{\partial v^d}{\partial y_1} d\mathbf{y} \quad \forall v \in Y(\Omega_{pc}) \,. \tag{1}$$

In Eq. (1), the space coordinates are $(y_1, y_2, y_3) = \mathbf{y}$, the differential surface and volume elements are, respectively, $d\mathbf{s}$ and $d\mathbf{y} = dy_1 dy_2 dy_3$, the function space Y is defined as $Y(\Omega_{pc}) = \{w |\, w_{|\Omega_{pc,c}} = w^c \in H^1_\#(\Omega_{pc,c}), w_{|\Omega_{pc,d}} = w^d \in H^1_\#(\Omega_{pc,d}), [w]_\Gamma = s \in I\!R, \int_{\Omega_{pc,c}} w^c\, d\mathbf{y} + \int_{\Omega_{pc,d}} w^d\, d\mathbf{y} = 0\}$, and $H^1_\#(\Omega_{pc})$ is the space of all λ-triply periodic functions in Ω_{pc} for which both the function and derivative are square-integrable over Ω_{pc}. The interface between the phases inside the periodic cell is denoted by Γ, and the square-bracket notation $[w]_\Gamma$ is used to represent the discontinuity $(w^c - w^d)$ of the function w at Γ. Finally, due to the assumed isotropy of the composite, the external temperature gradient is arbitrarily set in the y_1-direction. The surface integral term on the left-hand side of Eq. (1) accounts for the effect on the field χ of the contact resistance at the interface Γ.

Once the temperature field χ of Eq. (1) has been found for the particular cell configuration of the composite, the corresponding scalar effective thermal conductivity, k_e, can be computed from the following expression (details in Rocha and Cruz, 2001)

$$k_e = \frac{1}{|\Omega_{pc}|} \left\{ \int_{\Omega_{pc,c}} \left(1 - \frac{\partial \chi^c}{\partial y_1}\right) d\mathbf{y} + \int_{\Omega_{pc,d}} \alpha \left(1 - \frac{\partial \chi^d}{\partial y_1}\right) d\mathbf{y} \right\} , \tag{2}$$

where $|\Omega_{pc}| \equiv \int_{\Omega_{pc}} d\mathbf{y}$ is the nondimensional volume of the periodic cell (here equal to 1), and k_e is nondimensionalized with respect to k_c.

4. Three-Dimensional Isoparametric Finite-Element Discretization Scheme

In this section, we proceed to describe in detail our three-dimensional isoparametric finite-element discretization scheme to treat the surface integral term in Eq. (1), which arises due to the presence of an interfacial thermal resistance between the constituent phases of the composite material. Discretization of the cell problem, with its volume terms and the surface integral term, is effected using isoparametric 10-node tetrahedra (Hughes, 1987). We know from finite element theory that the discretization of the variational form of a boundary value problem leads to an equivalent discrete linear system of algebraic equations. This set of linear algebraic equations may be solved by iterative procedures: the conjugate gradient method (e.g., Matt and Cruz, 2001), appropriate when the global system matrix is sparse, symmetric and positive-definite; the minimum residual method (Paige and Saunders, 1975), appropriate when the global system matrix is sparse and symmetric.

For our purposes, the field variable of interest inside the periodic cell is the periodic temperature field $\chi(\mathbf{y})$, $\chi(\mathbf{y}) \in Y(\Omega_{pc})$. In the following, we first describe the main steps to discretize the two volume terms in the cell problem, and then the finite-element discretization of the surface integral term. We can rewrite Eq. (1) in the following manner

$$a(v, \chi) + b_\Gamma(v, \chi) = \ell(v) \quad \forall v \in Y(\Omega_{pc}), \tag{3}$$

where $a(v,\chi) \equiv \int_{\Omega_{pc}} f(\mathbf{y})\, (\partial\chi/\partial y_j)\, (\partial v/\partial y_j)\, d\mathbf{y}$ and $b_\Gamma(v,\chi) \equiv \int_\Gamma \mathrm{Bi}\, [v]_\Gamma\, [\chi]_\Gamma\, d\mathbf{s}$ are symmetric bilinear forms, $\ell(v) \equiv \int_{\Omega_{pc}} f(\mathbf{y})\, (\partial v/\partial y_1)\, d\mathbf{y}$ is a linear functional, and $f(\mathbf{y}) = 1$ if $\mathbf{y} \in \Omega_{pc,c}$, and $f(\mathbf{y}) = \alpha$ if $\mathbf{y} \in \Omega_{pc,d}$.

The finite element discretization begins with the subdivision of Ω_{pc} into N_e nonoverlapping conforming tetrahedra $\mathcal{T}_k$, $k = 1, 2, \ldots, N_e$. Therefore, the periodic cell domain Ω_{pc} is transformed into its discrete equivalent $\Omega_{pc,h} = \cup_{k=1}^{N_e} \mathcal{D}(\mathcal{T}_k)$, which is the union of the domains $\mathcal{D}(\mathcal{T}_k)$ associated with each tetrahedron $\mathcal{T}_k$, $k = 1, 2, \ldots, N_e$. In the Galerkin approximation (Hughes, 1987), we expand both the test, $\chi(\mathbf{y})$, and the weight, $v(\mathbf{y})$, functions as linear combinations of the interpolation functions, $\phi_i(\mathbf{y})$, $i = 1, 2, \ldots, N_{gn}$, where N_{gn} is the total number of global nodes. The interpolation functions are constructed such that $\phi_i(\mathbf{y}_j) = \delta_{ij}$, $i, j = 1, 2, \ldots, N_{gn}$, and $\mathbf{y}_j$ is the set of coordinates (y_1, y_2, y_3) of node j. The Galerkin approximation to Eq. (3) can thus be expressed as

$$a(v_h, \chi_h) + b_\Gamma(v_h, \chi_h) = \ell(v_h) \quad \forall v_h \in Y_h(\Omega_{pc,h}), \tag{4}$$

where χ_h and v_h are, respectively, the discrete approximations to χ and v. We employ quadratic tetrahedra, such that the interpolation functions, $\phi_i(\mathbf{y})$, $i = 1, 2, \ldots, N_{gn}$, are the usual Lagrangian interpolants of second order (Hughes, 1987); $Y_h(\Omega_{pc,h}) = Y(\Omega_{pc,h}) \cap \{w_{|\mathcal{T}_k} \in \mathcal{P}_2(\mathcal{T}_k)\}$, and $\mathcal{P}_2(\mathcal{T}_k)$, $k = 1, 2, \ldots, N_e$, is the space of all polynomials of degree 2 defined on tetrahedron $\mathcal{T}_k$. In other words, we use the same interpolation functions (quadratic) for the approximation of both the solution and geometry (second order isoparametric mapping). It is important to note that Γ in Eq. (4) is strictly Γ_h, the discrete quadratic approximation to the interface; however, henceforth we use Γ for simplicity of notation.

As exposed in Rocha and Cruz (2001) and in Matt and Cruz (2001), to account for the jumps of the temperature field and of the weight function at the interface, each global – corner and midside – node on the interface Γ must store two values of χ_h: one corresponding to the continuous phase, $\chi_h^c|_\Gamma$, and the other corresponding to the dispersed phase, $\chi_h^d|_\Gamma$, such that the jump $[\chi_h]_\Gamma$ is given by $\chi_h^c|_\Gamma - \chi_h^d|_\Gamma$. Therefore, as shown schematically in Fig. (1), we must first duplicate the corner and midside nodes on Γ, and then modify accordingly the connectivity of the tetrahedra which have at least one node on Γ. For example, note that in Fig. (1) the corner nodes A, A' are in fact the same geometric node, however the degrees of freedom associated with these nodes, respectively χ_A and $\chi_{A'}$ are, in general, different from each other.

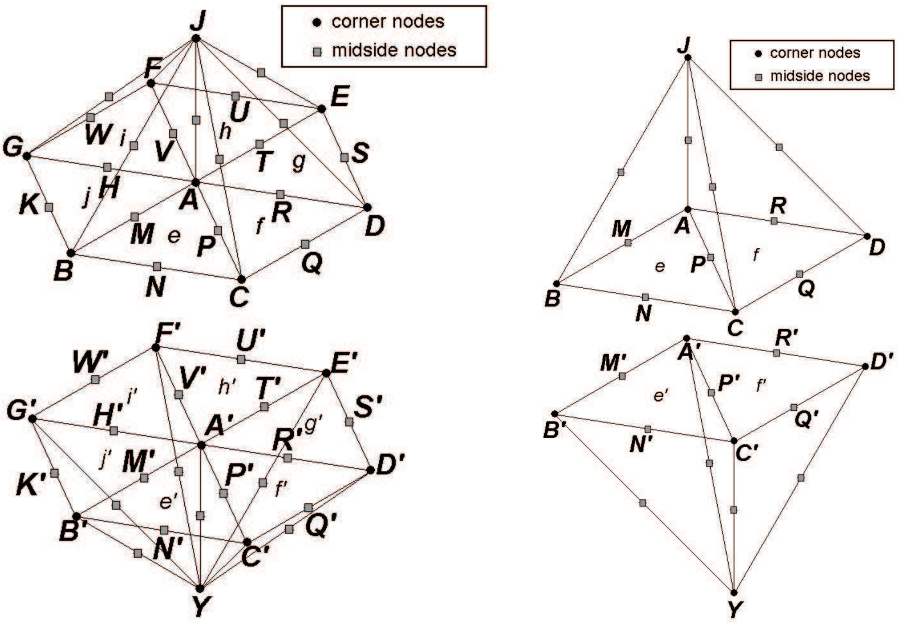

Figure 1: Duplication of degrees of freedom associated with global mesh nodes on the interface Γ.

4.1. Global nodes not on the interface

For the global – corner and midside – nodes *not on* Γ, we express the temperature field, χ_h, and the weight function, v_h, in Eq. (4) in terms of the usual Lagrangian interpolants of second order (Hughes, 1987). For these global nodes, the jumps $[\chi_h]_\Gamma$ and $[v_h]_\Gamma$ are equal to zero; therefore, $b_\Gamma(v_h, \chi_h) = 0$. Evaluating the resulting integrals numerically by Gaussian quadrature with five points (Bathe, 1982), we then obtain, for each degree of freedom associated with a global node not on Γ, the expressions for the entries in the global system matrix $\underline{\mathcal{K}}$ $(a(\phi_i, \phi_j))$ and in the global forcing vector $\underline{\mathcal{F}}$ $(\ell(\phi_i))$.

4.2. Global nodes on the interface

For the global – corner and midside – nodes *on* Γ, we use discontinuous weighting functions $v_h \in Y_h(\Omega_{pc,h})$, for which the jump s at the interface is nonzero, $[v_h]_\Gamma = s = \beta \in I\!R^*$. The contribution to $b_\Gamma(v_h, \chi_h)$, due to the degree of freedom at a global node on Γ, is dependent on the Biot number and on the areas of the curved tetrahedra faces lying on Γ and sharing the global node. For example, for the generic corner node A (whose degree of freedom is χ_A) in Fig. (1), situated to the continuous phase side of Γ and shared by, say, six tetrahedra, the contribution due to χ_A depends on the areas of the curved surfaces S_{ABC}, S_{ACD}, S_{ADE}, S_{AEF}, S_{AFG} and S_{AGB}. For the generic midside node P (whose degree of freedom is χ_P) in Fig. (1), situated to the continuous phase side of Γ and (always) shared by two tetrahedra, the contribution due to χ_P depends on the areas of the curved surfaces S_{ABC} and S_{ACD}. We remark that only the tetrahedra which have exactly three *corner* nodes on the interface, will contribute to the term $b_\Gamma(v_h, \chi_h)$.

The procedure to incorporate the contributions due to the term $b_\Gamma(v_h, \chi_h)$ in Eq. (4) to the global stiffness matrix $\underline{\mathcal{K}}$ will be now described, first for the generic corner node A, and then for the generic midside node P. The weighting function for A is $v_A = \beta \mathcal{N}_A^c \in Y_h(\Omega_{pc,h})$, where $\mathcal{N}_A^c$ is the standard quadratic interpolation function for A restricted to $\Omega_{pc,c}$. For implementation simplicity, we choose $\beta = 1$, such that $[v_A]_\Gamma = 1$ (Rocha and Cruz, 2001; Matt and Cruz, 2001). Now, introducing the function $v_A|_{e,\Gamma} = \mathcal{N}_A^c|_{e,\Gamma}$, which is the restriction of v_A to tetrahedron e (e is $\mathcal{T}_k$ for some k, $k = 1, 2, \ldots, N_e$) and to the interface Γ, the restriction of the discrete field χ_h to tetrahedron e and to Γ, $\chi_h^c|_{e,\Gamma}$, can then be written as

$$\chi_h^c|_{e,\Gamma} \;=\; \chi_A \mathcal{N}_A^c|_{e,\Gamma} + \chi_B \mathcal{N}_B^c|_{e,\Gamma} + \chi_C \mathcal{N}_C^c|_{e,\Gamma} + \chi_M \mathcal{N}_M^c|_{e,\Gamma} + \chi_N \mathcal{N}_N^c|_{e,\Gamma} + \chi_P \mathcal{N}_P^c|_{e,\Gamma}\,, \qquad (5)$$

where χ_A, χ_B, χ_C, χ_M, χ_N and χ_P, are, respectively, the values of χ_h^c at the global nodes A, B, C, M, N and P. The term $b_\Gamma(v_h, \chi_h)$ is evaluated through numerical integration of the discontinuities of v_h and χ_h across Γ; therefore, to compute the contribution to $b_\Gamma(v_h, \chi_h)$ of the discontinuities across the curved surface of tetrahedron e on Γ, S_{ABC}, we must also consider the tetrahedron e' to the dispersed phase side of Γ, which shares with e the curved surface S_{ABC} (or, equivalently, $S_{A'B'C'}$). From our definition of v_A, it follows that

$v_A|_{e',\Gamma} = 0$. Similarly to Eq. (5), we have for the function χ_h restricted to tetrahedron e' and to the interface Γ,

$$\chi_h^d|_{e',\Gamma} = \chi_{A'}\mathcal{N}_{A'}^d|_{e',\Gamma} + \chi_{B'}\mathcal{N}_{B'}^d|_{e',\Gamma} + \chi_{C'}\mathcal{N}_{C'}^d|_{e',\Gamma} + \chi_{M'}\mathcal{N}_{M'}^d|_{e',\Gamma} + \chi_{N'}\mathcal{N}_{N'}^d|_{e',\Gamma} + \chi_{P'}\mathcal{N}_{P'}^d|_{e',\Gamma}\,, \tag{6}$$

where $\mathcal{N}_{A'}^d|_{e',\Gamma}$, $\mathcal{N}_{B'}^d|_{e',\Gamma}$, $\mathcal{N}_{C'}^d|_{e',\Gamma}$, $\mathcal{N}_{M'}^d|_{e',\Gamma}$, $\mathcal{N}_{N'}^d|_{e',\Gamma}$ and $\mathcal{N}_{P'}^d|_{e',\Gamma}$ are, respectively, the standard quadratic interpolation functions for A', B', C', M', N' and P' in the dispersed-phase domain, restricted to tetrahedron e' and to Γ. From Eqs. (5) and (6) and from the definition of the function $v_A|_{e,\Gamma}$, we are now able to compute the jumps of v_h and χ_h across $\Gamma_{ee'}$, which is the curved surface of tetrahedron e on Γ (or, equivalently, the curved surface of tetrahedron e' on Γ):

$$[v_A]_{\Gamma_{ee'}} = v_A|_{e,\Gamma} - v_A|_{e',\Gamma} = v_A|_{e,\Gamma} = \mathcal{N}_A^c|_{e,\Gamma}\,, \tag{7}$$

$$\begin{aligned}[\chi_h]_{\Gamma_{ee'}} = {} & \chi_A\mathcal{N}_A^c|_{e,\Gamma} + \chi_B\mathcal{N}_B^c|_{e,\Gamma} + \chi_C\mathcal{N}_C^c|_{e,\Gamma} + \chi_M\mathcal{N}_M^c|_{e,\Gamma} + \chi_N\mathcal{N}_N^c|_{e,\Gamma} + \chi_P\mathcal{N}_P^c|_{e,\Gamma} - \\ & \chi_{A'}\mathcal{N}_{A'}^d|_{e',\Gamma} - \chi_{B'}\mathcal{N}_{B'}^d|_{e',\Gamma} - \chi_{C'}\mathcal{N}_{C'}^d|_{e',\Gamma} - \chi_{M'}\mathcal{N}_{M'}^d|_{e',\Gamma} - \chi_{N'}\mathcal{N}_{N'}^d|_{e',\Gamma} - \chi_{P'}\mathcal{N}_{P'}^d|_{e',\Gamma}\,.\end{aligned} \tag{8}$$

It follows that the contribution to $b_\Gamma(v_h,\chi_h)$ due to the discontinuities of v_h and χ_h across the curved surface S_{ABC} shared by tetrahedra e and e' on Γ is given by

$$\begin{aligned}\int_{\Gamma_{ee'}} \mathrm{Bi}\,[v_A]_{\Gamma_{ee'}}[\chi_h]_{\Gamma_{ee'}}\,d\mathbf{s} = \mathrm{Bi}\Big(& \chi_A \int_{\Gamma_{ee'}} \mathcal{N}_A^c|_{e,\Gamma}\mathcal{N}_A^c|_{e,\Gamma}\,d\mathbf{s} + \chi_B \int_{\Gamma_{ee'}} \mathcal{N}_A^c|_{e,\Gamma}\mathcal{N}_B^c|_{e,\Gamma}\,d\mathbf{s} + \\ & \chi_C \int_{\Gamma_{ee'}} \mathcal{N}_A^c|_{e,\Gamma}\mathcal{N}_C^c|_{e,\Gamma}\,d\mathbf{s} + \chi_M \int_{\Gamma_{ee'}} \mathcal{N}_A^c|_{e,\Gamma}\mathcal{N}_M^c|_{e,\Gamma}\,d\mathbf{s} + \chi_N \int_{\Gamma_{ee'}} \mathcal{N}_A^c|_{e,\Gamma}\mathcal{N}_N^c|_{e,\Gamma}\,d\mathbf{s} + \\ & \chi_P \int_{\Gamma_{ee'}} \mathcal{N}_A^c|_{e,\Gamma}\mathcal{N}_P^c|_{e,\Gamma}\,d\mathbf{s} - \chi_{A'} \int_{\Gamma_{ee'}} \mathcal{N}_A^c|_{e,\Gamma}\mathcal{N}_{A'}^d|_{e',\Gamma}\,d\mathbf{s} - \chi_{B'} \int_{\Gamma_{ee'}} \mathcal{N}_A^c|_{e,\Gamma}\mathcal{N}_{B'}^d|_{e',\Gamma}\,d\mathbf{s} - \\ & \chi_{C'} \int_{\Gamma_{ee'}} \mathcal{N}_A^c|_{e,\Gamma}\mathcal{N}_{C'}^d|_{e',\Gamma}\,d\mathbf{s} - \chi_{M'} \int_{\Gamma_{ee'}} \mathcal{N}_A^c|_{e,\Gamma}\mathcal{N}_{M'}^d|_{e',\Gamma}\,d\mathbf{s} - \chi_{N'} \int_{\Gamma_{ee'}} \mathcal{N}_A^c|_{e,\Gamma}\mathcal{N}_{N'}^d|_{e',\Gamma}\,d\mathbf{s} - \\ & \chi_{P'} \int_{\Gamma_{ee'}} \mathcal{N}_A^c|_{e,\Gamma}\mathcal{N}_{P'}^d|_{e',\Gamma}\,d\mathbf{s}\Big)\,.\end{aligned} \tag{9}$$

For the corner node A depicted in Fig. (1), five more equations similar to Eq. (9) must be written for the contributions to $b_\Gamma(v_h,\chi_h)$ due to the discontinuities of v_h and χ_h across the curved surfaces, on Γ, shared by tetrahedra f and f', g and g', h and h', i and i', and j and j'.

Referring to Fig. (1), the weighting function for the midside node P is $v_P = \beta\mathcal{N}_P^c \in Y_h(\Omega_{pc,h})$, where again $\mathcal{N}_P^c$ is the usual quadratic interpolation function for P restricted to $\Omega_{pc,c}$. Defining the function $v_P|_{e,\Gamma} = \mathcal{N}_P^c|_{e,\Gamma}$ as the restriction of v_P to tetrahedron e and to the interface Γ, the restriction of the discrete field χ_h to tetrahedron e and to Γ, $\chi_h^c|_{e,\Gamma}$, can then be written as

$$\chi_h^c|_{e,\Gamma} = \chi_A\mathcal{N}_A^c|_{e,\Gamma} + \chi_B\mathcal{N}_B^c|_{e,\Gamma} + \chi_C\mathcal{N}_C^c|_{e,\Gamma} + \chi_M\mathcal{N}_M^c|_{e,\Gamma} + \chi_N\mathcal{N}_N^c|_{e,\Gamma} + \chi_P\mathcal{N}_P^c|_{e,\Gamma}\,. \tag{10}$$

As for corner node A, to compute the contribution to $b_\Gamma(v_h,\chi_h)$ of the discontinuities across the curved surface of tetrahedron e on Γ, S_{ABC}, we must also consider the tetrahedron e' to the dispersed phase side of Γ, which shares with e the curved surface S_{ABC}. From our definition of v_P, it follows that $v_P|_{e',\Gamma} = 0$. Similarly to Eq. (10), we have for the function χ_h restricted to tetrahedron e' and to the interface Γ,

$$\chi_h^d|_{e',\Gamma} = \chi_{A'}\mathcal{N}_{A'}^d|_{e',\Gamma} + \chi_{B'}\mathcal{N}_{B'}^d|_{e',\Gamma} + \chi_{C'}\mathcal{N}_{C'}^d|_{e',\Gamma} + \chi_{M'}\mathcal{N}_{M'}^d|_{e',\Gamma} + \chi_{N'}\mathcal{N}_{N'}^d|_{e',\Gamma} + \chi_{P'}\mathcal{N}_{P'}^d|_{e',\Gamma}\,. \tag{11}$$

Computing the jumps of v_h and χ_h across $\Gamma_{ee'}$, and calculating the contribution to $b_\Gamma(v_h,\chi_h)$ due to the discontinuities of v_h and χ_h across the curved surface S_{ABC} shared by tetrahedra e and e' on Γ, we have

$$\begin{aligned}\int_{\Gamma_{ee'}} \mathrm{Bi}\,[v_P]_{\Gamma_{ee'}}[\chi_h]_{\Gamma_{ee'}}\,d\mathbf{s} = \mathrm{Bi}\Big(& \chi_A \int_{\Gamma_{ee'}} \mathcal{N}_P^c|_{e,\Gamma}\mathcal{N}_A^c|_{e,\Gamma}\,d\mathbf{s} + \chi_B \int_{\Gamma_{ee'}} \mathcal{N}_P^c|_{e,\Gamma}\mathcal{N}_B^c|_{e,\Gamma}\,d\mathbf{s} + \\ & \chi_C \int_{\Gamma_{ee'}} \mathcal{N}_P^c|_{e,\Gamma}\mathcal{N}_C^c|_{e,\Gamma}\,d\mathbf{s} + \chi_M \int_{\Gamma_{ee'}} \mathcal{N}_P^c|_{e,\Gamma}\mathcal{N}_M^c|_{e,\Gamma}\,d\mathbf{s} + \chi_N \int_{\Gamma_{ee'}} \mathcal{N}_P^c|_{e,\Gamma}\mathcal{N}_N^c|_{e,\Gamma}\,d\mathbf{s} + \\ & \chi_P \int_{\Gamma_{ee'}} \mathcal{N}_P^c|_{e,\Gamma}\mathcal{N}_P^c|_{e,\Gamma}\,d\mathbf{s} - \chi_{A'} \int_{\Gamma_{ee'}} \mathcal{N}_P^c|_{e,\Gamma}\mathcal{N}_{A'}^d|_{e',\Gamma}\,d\mathbf{s} - \chi_{B'} \int_{\Gamma_{ee'}} \mathcal{N}_P^c|_{e,\Gamma}\mathcal{N}_{B'}^d|_{e',\Gamma}\,d\mathbf{s} - \\ & \chi_{C'} \int_{\Gamma_{ee'}} \mathcal{N}_P^c|_{e,\Gamma}\mathcal{N}_{C'}^d|_{e',\Gamma}\,d\mathbf{s} - \chi_{M'} \int_{\Gamma_{ee'}} \mathcal{N}_P^c|_{e,\Gamma}\mathcal{N}_{M'}^d|_{e',\Gamma}\,d\mathbf{s} - \chi_{N'} \int_{\Gamma_{ee'}} \mathcal{N}_P^c|_{e,\Gamma}\mathcal{N}_{N'}^d|_{e',\Gamma}\,d\mathbf{s} - \\ & \chi_{P'} \int_{\Gamma_{ee'}} \mathcal{N}_P^c|_{e,\Gamma}\mathcal{N}_{P'}^d|_{e',\Gamma}\,d\mathbf{s}\Big).\end{aligned} \tag{12}$$

For the midside node P depicted in Fig. (1), one more equation similar to Eq. (12) must be written for the contribution to $b_\Gamma(v_h, \chi_h)$ due to the discontinuities of v_h and χ_h across the curved surface, on Γ, shared by tetrahedra f and f'.

The calculation procedure described above (for corner node A and midside node P) to determine the contributions to $b_\Gamma(v_h, \chi_h)$ of the discontinuities of v_h and χ_h across the curved surfaces on Γ that share the same corner or midside node, must be repeated for all the other corner and midside nodes at the interface. All the resulting surface integrals, such as those in Eqs. (9) and (12), can be calculated using numerical integration techniques (Hughes, 1987), and are related to the areas of the curved surfaces involved. In this work, we use Gaussian quadrature (Bathe, 1982).

Finally, such contributions to $b_\Gamma(v_h, \chi_h)$ must be summed to $a(\phi_i, \phi_j)$, $i, j = 1, 2, \ldots, N_{gn}$, at the appropriate entries of the global system matrix $\underline{\mathcal{K}}$. For example, in the line of $\underline{\mathcal{K}}$ corresponding to degree of freedom χ_A, we must sum contributions to entries $\mathcal{K}_{AA}$, $\mathcal{K}_{AA'}$, $\mathcal{K}_{AB}$, $\mathcal{K}_{AB'}$, $\mathcal{K}_{AC}$, $\mathcal{K}_{AC'}$, $\mathcal{K}_{AD}$, $\mathcal{K}_{AD'}$, $\mathcal{K}_{AE}$, $\mathcal{K}_{AE'}$, $\mathcal{K}_{AF}$, $\mathcal{K}_{AF'}$, $\mathcal{K}_{AG}$, $\mathcal{K}_{AG'}$, $\mathcal{K}_{AM}$, $\mathcal{K}_{AM'}$, $\mathcal{K}_{AP}$, $\mathcal{K}_{AP'}$, $\mathcal{K}_{AR}$, $\mathcal{K}_{AR'}$, $\mathcal{K}_{AT}$, $\mathcal{K}_{AT'}$, $\mathcal{K}_{AV}$, $\mathcal{K}_{AV'}$, $\mathcal{K}_{AH}$, $\mathcal{K}_{AH'}$, $\mathcal{K}_{AN}$, $\mathcal{K}_{AN'}$, $\mathcal{K}_{AQ}$, $\mathcal{K}_{AQ'}$, $\mathcal{K}_{AS}$, $\mathcal{K}_{AS'}$, $\mathcal{K}_{AU}$, $\mathcal{K}_{AU'}$, $\mathcal{K}_{AW}$, $\mathcal{K}_{AW'}$, $\mathcal{K}_{AK}$ and $\mathcal{K}_{AK'}$. In the line of $\underline{\mathcal{K}}$ corresponding to degree of freedom χ_P, we must sum contributions to entries $\mathcal{K}_{PP}$, $\mathcal{K}_{PP'}$, $\mathcal{K}_{PM}$, $\mathcal{K}_{PM'}$, $\mathcal{K}_{PN}$, $\mathcal{K}_{PN'}$, $\mathcal{K}_{PR}$, $\mathcal{K}_{PR'}$, $\mathcal{K}_{PQ}$, $\mathcal{K}_{PQ'}$, $\mathcal{K}_{PA}$, $\mathcal{K}_{PA'}$, $\mathcal{K}_{PB}$, $\mathcal{K}_{PB'}$, $\mathcal{K}_{PC}$, $\mathcal{K}_{PC'}$, $\mathcal{K}_{PD}$ and $\mathcal{K}_{PD'}$. These contributions are proportional to the Biot number Bi, such that the resulting global system matrix $\underline{\mathcal{K}}^*$, although still symmetric, is not necessarily positive-definite for arbitrary values of Bi. Of course, the number of tetrahedra sharing a corner node on Γ varies in an unstructured 3-D finite-element mesh, and the procedure described above can easily accomodate such variations. The number of tetrahedra, with exact three corner nodes on Γ, that share one corner node on Γ ranges from four to seven in our 3-D mesh generation procedure using NETGEN (Schöberl, 2001).

The resulting linear system of algebraic equations can be written as

$$\underline{\mathcal{K}}^* \, \underline{\chi}_h = \underline{\mathcal{F}} \, , \tag{13}$$

where $\underline{\chi}_h$ is the vector of unknown values of the field χ_h. The uniqueness condition, given in continuous form in the definition of the space $Y(\Omega_{pc})$, is imposed discretely by requiring that $\underline{\chi}_h$ have zero algebraic average. The system given by Eq. (13) is iteratively solved by the *minimum residual method*, described in detail by Paige and Saunders (1975), which is suitable for symmetric sparse systems of linear equations. The iteration proceeds until the square of the ratio of the Euclidean norm of the residual to the Euclidean norm of the initial residual falls below a user-prescribed tolerance, σ^2.

Finally, after numerical determination of the field χ_h , the numerical value of the effective thermal conductivity, k_e^{N}, is computed by substituting χ_h for χ in Eq. (2),

$$k_e^{\mathrm{N}} \;=\; \frac{1}{|\Omega_{pc,h}|} \int_{\Omega_{pc,h}} f_h(\mathbf{y}) \left(1 - \frac{\partial \chi_h}{\partial y_1} \right) d\mathbf{y} \, , \tag{14}$$

where $f_h(\mathbf{y}) = 1$ for tetrahedra inside the matrix domain, and $f_h(\mathbf{y}) = \alpha$ for tetrahedra inside the dispersed-phase domain.

5. Case Study

In this section, in order to demonstrate the validity and flexibility of our scheme, we present sample numerical results for a particular case study: we effect truly three-dimensional calculations of the effective conductivity of the simple cubic array of spheres. Our numerical results, k_e^{N}, are then compared and validated against the (semi-)analytical results obtained by Cheng and Torquato (1997), k_e^{CT}. The case study and associated computations are described below.

Table 1: Values of the effective conductivity for fixed values of c, α, and mesh spacing.

$c = 0.20$, $\alpha = 2$, mesh spacing set to 0.10		
Bi	k_e^{CT}	k_e^{N}
0.01	0.7280	0.7286
10	1.054	1.056
100	1.145	1.147

Finite element solution of the cell problem, Eq. (1), in a particular domain requires three steps: geometry and mesh generation, finite element discretization and solution of the resultant linear system of algebraic equations. The physical domain for our case study is the periodic cell Ω_{pc} for the simple cubic array of spheres, composed of a cube and a geometrically centered sphere, as illustrated in Fig. (2). The semi-automatic procedure to

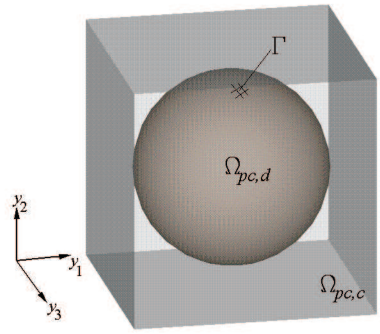

Fig. 2: Geometry of the periodic cell for the simple cubic array of spheres and associated Cartesian coordinate system.

generate unstructured quadratic tetrahedral meshes inside Ω_{pc} is an adaptation of the one described in detail by Matt and Cruz (2001), and is based on the software NETGEN (Schöberl, 2001). For illustrative purposes, a vertical y_1-y_2 cut of a tetrahedral mesh generated with a uniform mesh spacing of 0.05 is shown in Fig. (3), for the concentration value $c = 0.20$. As described in section 4, the system of equations resulting from the discretization process for the simple-cubic cell problem is solved using the minimum residual method.

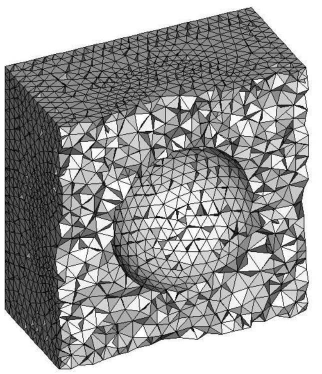

Fig. 3: Vertical y_1-y_2 cut of a tetrahedral mesh generated in the simple-cubic cell for $c = 0.20$ and mesh spacing of 0.05 (the tetrahedra inside the sphere have been removed for better visualization).

Table 2: Values of the effective conductivity for fixed values of c, α, and Bi.

$c = 0.20$, $\alpha = 2$, $Bi = 0.01$		
mesh spacing	k_e^{CT}	k_e^{N}
0.10	0.7280	0.7286
0.05	0.7280	0.7283
0.04	0.7280	0.7282

In Tables 1 and 2 we show the computed values k_e^{N} and the corresponding values k_e^{CT} (Cheng and Torquato, 1997) for the following specific data: concentration $c = 0.20$, conductivity ratio $\alpha = 2$, and Biot number $Bi \in \{0.01, 10, 100\}$. All the results have been obtained using the tolerance $\sigma = 10^{-4}$ and (coarse) uniform mesh spacings. The chosen values of σ and mesh spacings ensure: (i) that the meshes generated for the case study possess no sliver elements (Batdorf et al., 1997), and (ii) that the numerical results are correct to 3-4 significant digits. First, we observe in Table 1 that the computed values k_e^{N} agree well with those of Cheng and Torquato (1997) even for a coarse mesh spacing, for all values of Bi. And second, we observe in Table 2 that k_e^{N} approaches k_e^{CT} as the uniform mesh spacing decreases, which demonstrates the success of our scheme implementation.

6. Conclusions

We have successfully developed a new three-dimensional isoparametric finite-element discretization scheme to treat the interfacial thermal resistance in composite materials. We have demonstrated the validity and flexibility of our scheme by effecting truly three-dimensional sample calculations of the effective conductivity of an ordered-array composite, for which reference results are known. The scheme presented here, compared to previous approaches, has the distinct advantage of being applicable to complex and realistic microstructures, such as transversely-aligned short-fibers (Matt, 2003). It is thus expected that the scheme in hand will have a much greater potential to more closely reproduce experimental findings (e.g., Mirmira and Fletcher, 1999; Every et al., 1992).

7. Acknowledgements

C. F. Matt and M. E. Cruz would like to gratefully acknowledge the support of the Brazilian Council for Development of Science and Technology (CNPq) through Grants 140470/99-9 and 521002/97-4. The authors would also like to thank Dr. Joachim Schöberl, from Johannes Kepler Universität Linz, Austria, for freely licensing NETGEN for academic use.

8. References

Auriault, J.-L., 1991, Heterogeneous Medium. Is an Equivalent Macroscopic Description Possible?, "Int. J. Engrg. Sci.", Vol. 29, pp. 785–795.

Auriault, J.-L. and Ene, H. I., 1994, Macroscopic Modelling of Heat Transfer in Composites with Interfacial Thermal Barrier, "Int. J. Heat Mass Transfer", Vol. 37, pp. 2885–2892.

Batdorf, M., Freitag, L. A., and Gooch, C. O., 1997, Computational Study of the Effect of Unstructured Mesh Quality on Solution Efficiency, "Proceedings of the 13^{th} AIAA Computational Fluid Dynamics Conference", Snowmass, CO.

Bathe, K. J., 1982, "Finite Element Procedures in Engineering Analysis", eds. Prentice-Hall, Inc., Englewood Cliffs, NJ.

Bensoussan, A., Lions, J.-L., and Papanicolaou, G., 1978, "Asymptotic Analysis for Periodic Structures", North-Holland, Amsterdam.

Benveniste, Y., 1987, Effective thermal conductivity of composites with a thermal contact resistance between the constituents: Nondilute case, "J. Appl. Phys.", Vol. 61, pp. 2840–2843.

Cheng, H. and Torquato, S., 1997, Effective conductivity of periodic arrays of spheres with interfacial resistance, "Proc. R. Soc. Lond. A", Vol. 453, pp. 145–161.

Cruz, M. E., 2001, Computational approaches for heat conduction in composite materials, "Computational Methods and Experimental Measurements X", eds. Y. V. Esteve, G. M. Carlomagno and C. A. Brebbia, pp. 657-668, WIT Press, Ashurst, Southampton, UK.

Cruz, M. E. and Patera, A. T., 1995, A Parallel Monte-Carlo Finite-Element Procedure for the Analysis of Multicomponent Random Media, "Int. J. Numer. Methods Engrg.", Vol. 38, pp. 1087–1121.

Every, A. G., Tzou, Y., Hasselman, D. P. H., and Raj, R., 1992, The Effect of Particle Size on the Thermal Conductivity of ZnS/Diamond Composites, "Acta Metall. Mater.", Vol. 40, pp. 123–129.

Fletcher, L. S., 1988, Recent Developments in Contact Conductance Heat Transfer, "Trans. ASME, J. Heat Transfer", Vol. 110, pp. 1059–1070.

Furmañski, P., 1997, Heat conduction in composites: Homogenization and macroscopic behavior, "Appl. Mech. Rev.", Vol. 50, pp. 327–356.

Hasselman, D. P. H. and Johnson, L. F., 1987, Effective Thermal Conductivity of Composites with Interfacial Thermal Barrier Resistance, "J. Composite Materials", Vol. 21, pp. 508–515.

Hughes, T. J. R., 1987, "The Finite Element Method", Prentice-Hall, Inc., Englewood Cliffs, NJ.

Ingber, M. S., Womble, D. E., and Mondy, A. A., 1994, A Parallel Boundary Element Formulation for Determining Effective Properties of Heterogeneous Media, "Int. J. Numer. Methods Engrg.", Vol. 37, pp. 3905–3920.

James, B. W. and Keen, G. S., 1985, A Nomogram for the Calculation of the Transverse Thermal Conductivity of Uniaxial Composite Lamina, "High Temperatures, High Pressures", Vol. 17, pp. 477–480.

Lipton, R. and Vernescu, B., 1996, Composites with imperfect interface, "Proc. R. Soc. Lond. A", Vol. 452, pp. 329–358.

Matt, C. F., 2003, "A Computational Approach for the Study of Heat Conduction in Three-Dimensional Composites (in Portuguese)", PhD thesis, COPPE/Federal University of Rio de Janeiro, Rio de Janeiro, Brazil.

Matt, C. F. and Cruz, M. E., 2001, Calculation of the Effective Conductivity of Ordered Short-Fiber Composites, "Proceedings of the 35th AIAA Thermophysics Conference", pp. 1–11, Paper AIAA 2001-2968, Anaheim, California.

Mirmira, S. R., 1999, "Effective Thermal Conductivity of Fibrous Composites: Experimental and Analytical Study", PhD thesis, Texas A&M University, Texas.

Mirmira, S. R. and Fletcher, L. S., 1999, Comparative Study of Thermal Conductivity of Graphite Fiber Organic Matrix Composites, "Proceedings of the 5th ASME/JSME Joint Thermal Engineering Conference", pp. 1–8, Paper AJTE99-6439, San Diego, CA.

Paige, C. C. and Saunders, M. A., 1975, Solution of Sparse Indefinite Systems of Linear Equations, "SIAM J. Numer. Anal.", Vol. 12, pp. 617–629.

Perrins, W. T., McKenzie, D. R., and McPhedran, R. C., 1979, Transport properties of regular arrays of cylinders, "Proc. R. Soc. Lond. A", Vol. 369, pp. 207–225.

Rocha, R. P. A. and Cruz, M. E., 2001, Computation of the Effective Conductivity of Unidirectional Fibrous Composites with an Interfacial Thermal Resistance, "Num. Heat Transfer, Part A", Vol. 39, pp. 179–203.

Rolfes, R. and Hammerschmidt, U., 1995, Transverse Thermal Conductivity of CFRP Laminates: A Numerical and Experimental Validation of Approximation Formulae, "Composites Science and Technology", Vol. 54, pp. 45–54.

Schöberl, J., 2001, "NETGEN - 4.0", Numerical and Symbolic Scientific Computing, Johannes Kepler Universität Linz, Austria.

Torquato, S., 1991, Random heterogeneous media: Microstructure and improved bounds on effective properties, "Appl. Mech. Rev.", Vol. 44, pp. 37–76.